Anal Bioanal Chem (2011) 401:3317–3334
DOI 10.1007/s00216-011-5406-4

ORIGINAL PAPER

"Dilute-and-shoot" triple parallel mass spectrometry method for analysis of vitamin D and triacylglycerols in dietary supplements

William Craig Byrdwell

Received: 21 June 2011 / Revised: 30 August 2011 / Accepted: 8 September 2011 / Published online: 2 October 2011

Abstract A method is demonstrated for analysis of vitamin D fortified dietary supplements that eliminates virtually all chemical pretreatment prior to analysis, which is referred to as a "dilute-and-shoot" method. Three mass spectrometers, in parallel, plus a UV detector, an evaporative light-scattering detector (ELSD), and a corona charged aerosol detector (CAD) were used to allow a comparison of six detectors simultaneously. Ultraviolet data were analyzed using internal standard, external standard, and response factor approaches. The contents of gelcaps that contained 2,000 IU (50 μg) vitamin D_3 in rice bran oil, diluted to 100 mL, were analyzed without the need for lengthy saponification and extraction. Vitamin D_3 was analyzed using UV detection, extracted ion chromatograms, selected ion monitoring (SIM) atmospheric pressure chemical ionization mass spectrometry (APCI-MS), and two transitions of multiple reaction monitoring (MRM) APCI-MS. The internal standard, external standard, and response factor methods gave values of 0.5870±0.0045, 0.5893±0.0041, and 0.5889±0.0045 μg/mL, respectively, by UV detection. The values obtained by MS were 0.6117±0.0140, 0.6018±0.0244, and 0.5848±0.0146 μg/mL by SIM and two transitions of MRM, respectively. The triacylglycerols in the oils were analyzed using full-scan APCI-MS, electrospray ionization (ESI) MS, up to MS^4, an ELSD, and a CAD. The method proved to be very sensitive for vitamin D_3, as well as triacylglycerols (TAGs), allowing identification of intact TAGs containing fatty acids up to 28 carbons in length. LC-ESI-MS of glycerin polymers is also demonstrated.

Keywords Vitamin D · Cholecalciferol · Ergocalciferol · Calciol · APCI-MS · ESI-MS

Introduction

Vitamin D deficiency has long been associated with development of rickets, and recognition of this link led to fortification of milk and other foods, which virtually eliminated the disease [1]. In recent years, numerous other health outcomes have been postulated to be associated with vitamin D deficiency, although a recent meta-analysis reported inconsistent results related to most disease outcomes [2]. Nevertheless, it is generally recognized that a substantial proportion of not only the US population but also that of many other countries, is inadequate in vitamin D [3], based on analysis of the 25-OH vitamin D metabolite used as the principal biomarker for the nutrient. Thus, there is a widely recognized need to increase the amount of vitamin D in the diet. This recognition led to formation of a committee of the National Academies' Institute of Medicine to assess the adequacy of the current Dietary Reference Intake values for calcium and vitamin D, which reported updated recommendations in November, 2010 [4].

There are four primary sources for obtaining vitamin D: (1) cutaneous production from conversion of 7-dehydrocholesterol in the skin by sunlight; (2) eating foods naturally containing vitamin D; (3) eating foods fortified with vitamin D; and (4) taking dietary supplements that

Electronic supplementary material The online version of this article (doi:10.1007/s00216-011-5406-4) contains supplementary material, which is available to authorized users.

W. C. Byrdwell (✉)
Food Composition and Methods Development Laboratory,
USDA, Agricultural Research Service,
Beltsville Human Nutrition Research Center,
10300 Baltimore Ave. Bldg., 161,
Beltsville, MD 20704, USA
e-mail: C.Byrdwell@ars.usda.gov

include vitamin D. Unfortunately, cutaneous production falls off dramatically at higher latitudes and in winter months [5], so this cannot be considered a consistent and reliable source of vitamin D. Only a few foods naturally contain substantial amounts of vitamin D, the most notable being fatty fish and fish liver oils. Some foods are fortified with vitamin D, including milk and milk products, enriched corn meal, farina, rice, macaroni and noodle products, margarine, fruit juices, meal replacement bars, cheese, olestra-containing foods, and infant formula [6]. Therefore, it is often difficult to obtain the recommended amount of vitamin D from conventional dietary sources. Because of this, many people are turning to dietary supplements to obtain the recommended dietary reference intake of this important nutrient.

Unfortunately, there is very little analytical information available for vitamin D in dietary supplements, although one recent article [7] did report the levels of vitamin D in castor oil-based supplements. However, most available information on supplements must be taken from manufacturers' label claims. To address the general gap in knowledge regarding dietary supplements, the National Institutes of Health Office of Dietary Supplements funded the Dietary Supplement Ingredient Database at the USDA Agricultural Research Service. However, vitamin D values are not yet populated, partly because of the need for methodology development for vitamin D analysis in supplements. Even though some values for vitamin D in supplements will soon be available, there still exists a great need for improved methods for analysis of vitamin D in supplements.

Most methods for analysis of vitamin D, both in foods and supplements, involve: (1) a saponification step to break down complex lipids that interfere with the analysis, (2) an extraction step to partially clean up the sample and remove fatty acids (FAs) produced by the saponification, (3) a preparative chromatography step on a normal-phase (NP) high performance liquid chromatography (HPLC) instrument to isolate vitamin D (vitamin D_2 and vitamin D_3 typically co-elute by NP-HPLC), and (4) an analytical reversed-phase (RP) HPLC step to separate vitamin D_2 and vitamin D_3 for quantification. These methods are lengthy, labor intensive and require large amounts of resources (chemicals, extraction solvents, chromatography solvents, two dedicated liquid chromatographs, etc.).

We have developed a new method for analysis of dietary supplements in oils that completely eliminates the saponification, extraction, and preparative chromatography steps associated with conventional analyses. Sample pretreatment steps are almost completely eliminated, resulting in a "dilute-and-shoot" approach that requires only that the samples are weighed, an internal standard is added, and they are diluted to volume.

Materials and methods

Chemicals and samples

Water was obtained from a Millipore Milli-Q® purification system (Millipore, Bedford, MA, USA). Fisher Optima LC-MS grade methanol (MeOH), no. A456-4, and acetonitrile (ACN), no. A955-4, were used (Fisher Scientific, Pittsburgh, PA, USA). Methylene chloride (dichloromethane (DCM)), no. D151-4, was Fisher Optima grade. Ammonium formate (>99.995%), no. 516961, synthetic crystalline cholecalciferol, no. 1357, and synthetic crystalline ergocalciferol, no. 5750, were from Sigma-Aldrich Co. (St. Louis, MO, USA).

Dietary supplement gelcaps containing 1,000 (25 μg), 2,000 (50 μg), and 5,000 IU (125 μg) of vitamin D_3 in various oils were ordered from an online supplier of vitamins, were received unrefrigerated, and were stored refrigerated upon receipt, as would be typical for the average consumer. For this first report of the method, a dietary supplement containing 2,000 IU synthetic vitamin D_3 in rice bran oil (RBO) and one containing 1,000 IU vitamin D_3 in safflower oil with vitamin D_3 from fish oil were used as examples.

This method was designed to allow external standard, internal standard and response factor approaches to be used and compared. To allow the use of an external standard approach, standards were used that contained exactly 1,000 IU (25 μg; 1 IU=0.025 μg), 2,000 IU (50 μg), or 5,000 IU (125 μg) in 100 mL of sample diluent, which was the same as the label amounts in the supplements; and the supplement solutions were made with one whole gelcap in 100 mL of diluent. For the internal standard approach (and as a check for external standard peak areas), enough vitamin D_2 was added to yield exactly 2,000 IU in the 100 mL of all standards and sample solutions. Several approaches and variations of response factor calculations are reported.

Gelcaps were individually weighed, and the gelcap was scored along the seam at a narrow end using a razor blade, without puncturing. Then, the oil was removed by piercing the gelcap along the seam at the scored location, using a sharp 1.0 mL Hamilton syringe with a 22-gauge 2 in. needle (type 1001LTN, no. 81317; Hamilton Co., Reno, NV). Oil from a sacrificial gelcap was first drawn up and fully discharged to waste, to wet the interior surfaces of the syringe. Then, oil from each gelcap was drawn out and discharged into a tared 100 mL volumetric flask on the balance. The oil weight was obtained and the oil was immediately covered with sample solvent composed of 60% MeOH/40% DCM to minimize exposure to air; 2.0 mL of 25.0 μg/mL vitamin D_2 internal standard in sample solvent was added by glass volumetric pipet, and

samples were made to the 100.0 mL mark with sample solvent for a final concentration of 0.5000 μg/mL or 2,000 IU/100 mL. The 2,000 IU gelcaps with RBO had average oil weights of 0.15127±0.00144 (0.95%) g (n=5).

Three calibration solutions, containing 0.2500 (1,000 IU/100 mL), 0.5000 (2,000 IU/100 mL), and 1.250 μg/mL (5,000 IU/100 mL) vitamin D_3, plus with 0.5000 μg/mL vitamin D_2, were made in sample solvent. Calibration solutions were used for no more than approximately 1 month. All samples and standards were kept refrigerated until aliquots were transferred to amber autosampler vials for analysis.

Bracketed sequences were used that consisted of three calibration standards, followed by three sample replicates, which was repeated five times, for five gelcap samples, followed by a sixth set of standards, followed by one column cleanup run.

A solution of 50 mM ammonium formate in H_2O/ACN 1:4 was made by diluting 200 mL of 250 mM ammonium formate in water with 800 mL ACN. This served as the electrolyte solution to promote ion formation by electrospray ionization mass spectrometry (ESI-MS).

Liquid chromatography

An Agilent 1200 system was used that consisted of the solvent module with membrane degasser (G1379B), quaternary pump (G1311A), autosampler (G1329A), thermostatted column compartment (G1316A), diode array detector (DAD) SL (G1315C), and two-channel 24-bit analog-to-digital converter (ADC) (35900E). Two Inertsil ODS-2 columns in series, 25 cm×4.6 mm, 5 μm particles (GL Sciences, Torrance, CA, USA), joined by a circularly bent 7-cm piece of 0.007 in. i.d. stainless steel tubing were used. Columns were maintained at 10 °C throughout using the Agilent column temperature controller; 20 μL of standards and samples were injected. The dead time of the system was 5.0 min.

For gelcap samples, a ternary gradient of MeOH, ACN, and DCM was used, which consisted of: 0 to 27 min isocratic MeOH at 1.3 mL/min; steep gradient to 60% ACN/40% DCM at 0.9 mL/min at 28 min, held for 1 min; shallow gradient to 50% ACN/50% DCM at 95 min, held to 100 min; to 30% ACN/70% DCM at 110 min, held to 118 min; recycled to initial conditions at 120 min, held to stabilize for 10 min. For standards, isocratic methanol at 1.3 ml/min was used for 0 to 28 min. The column cleanup run at the end of the sequence consisted of: 100% MeOH at 1.3 mL/min, held for 1 min; steep gradient to 60% MeOH/40% ACN at 0.8 mL/min at 5 min; gradient to 20% ACN/80% DCM at 20 min, held until 60 min; recycled to initial conditions at 65 min, held for 5 min; flow stopped at 70.1 min.

The DAD SL, with standard flow cell (10 mm and 13 μL), was operated in single channel and full-scan modes, 265 (9 nm bandwidth (bw)) and 210 nm (5 nm bw), plus 190 to 400 nm (2 nm slit and bw). After the DAD, flow was split by a series of four Valco tees, joined by ~3.3 cm lengths of 0.005 in i.d. stainless steel tubing (for ~0.1 cm between nuts). A length of 100 μm i.d. deactivated fused silica tubing (no. 160-2635-10, Agilent, Inc., Santa Clara, CA, USA) was attached to the perpendicular branch of each tee by an adapting sleeve (Upchurch Scientific, Inc., Oak Harbor, WA, USA), and the distal end was attached to a stainless steel Valco union by an adapting sleeve. A 5-cm length of 0.005 in i.d. stainless steel tubing was attached to the outlet of each distal union, to facilitate attachment to the inlet of each detector or mass spectrometer. The lengths and flow rates (under initial conditions) from the set of tees were as follows (p=perpendicular port, s=straight-through port): (1p) 191 cm (192 μL/min); (2p) 122 cm (245 μL/min); (3p) 122 cm (244 μL/min); (4p) 90 cm (320 μL/min); (4s) 92 cm (314 μL/min).

A corona charged aerosol detector (CAD) (ESA, Inc., Chelmsford, MA, USA) was attached to the outlet of the second tee. The CAD detector was controlled by the Agilent Chemstation software, and used 1 pA full scale (f.s.)=1,000 mV for standards, 50 pA f.s.=1,000 mV for large gelcaps, and 5 pA f.s.=1,000 mV for small, gelcaps. Standards used a medium filter time constant, while all samples used no filter time constant. An evaporative light scattering detector (ELSD), model ELSD 800 (Alltech Associates, Waukegan, IL, USA), was attached to the outlet of the third tee. The ELSD was operated at 40 °C and 2.0 bar, with 1,000 mV f.s. at gain=1.

Signal from both the CAD and ELSD went to the Agilent 35900E ADC for acquisition by the Chemstation, and to an Agilent SS420X four-channel 24-bit ADC for acquisition by XCalibur software. Both detectors also were connected to a selector switch, and the CAD was selected to go to a single channel PCI-6032E 16-bit ADC card (National Instruments, Austin, TX, USA) in the Applied Biosystems acquisition computer for acquisition by Analyst software. Having the auxiliary detectors wired to three ADCs simultaneously allowed (1) signal to be acquired by any of the instruments and control software without the need for rewiring and (2) choice of the best software for processing (e.g., XCalibur handled negative peaks better than Chemstation).

A series of 12 center-off double-pole double-throw switches (Fig. 1) has been installed in our lab that distributes contact closures to allow reconfiguration of HPLC and MS combinations for a wide variety of LCxMSy experiments. This switching system is described in detail in the electronic supplementary material §2.2.1.

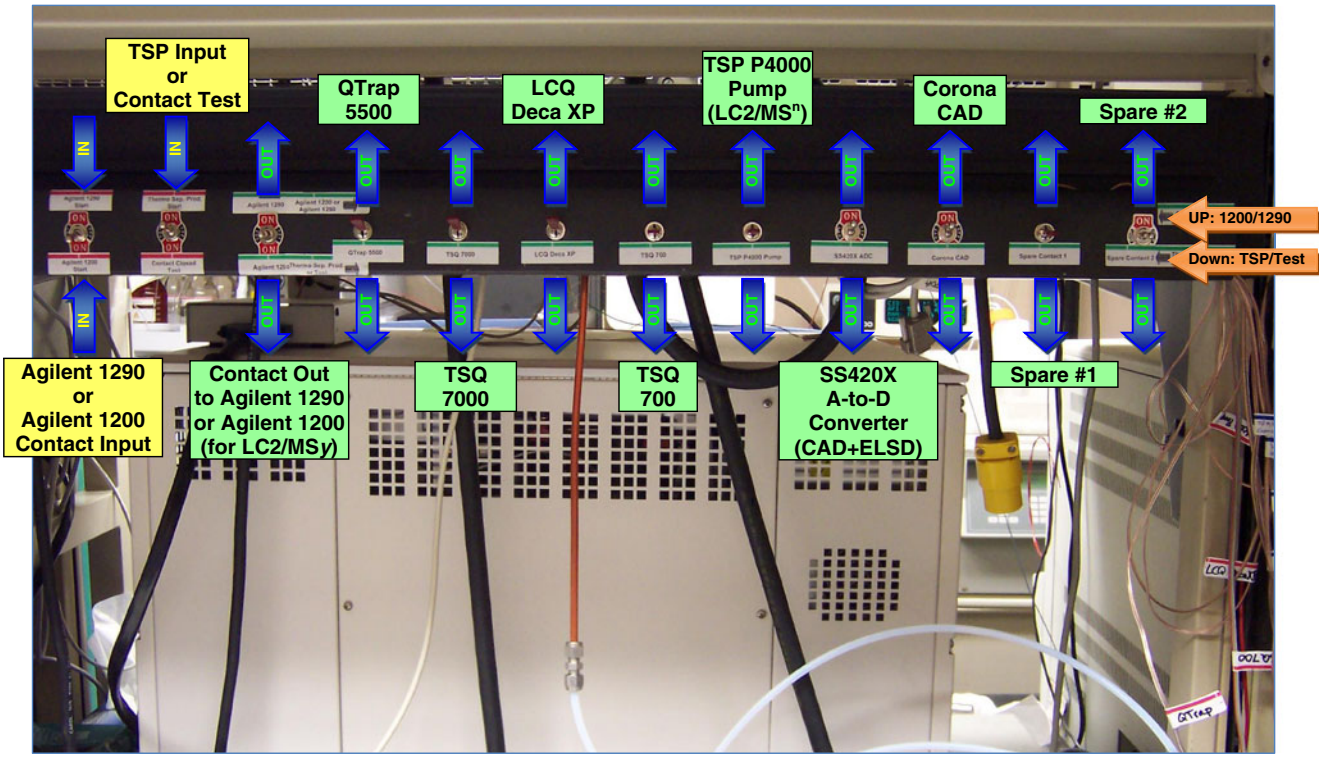

Fig. 1 Switching panel for selection of LC inputs and outputs to mass spectrometers, other detectors, and other LCs for LC1/MS1 to LC3/MS4 experiments

Mass spectrometry

SIM, MRM, and EMS by APCI-MS on QTrap 5500

A QTrap 5500 mass spectrometer (AB Sciex, Foster City, CA, USA) controlled by Analyst 1.5.1 was used to compare selected ion monitoring (SIM), and two transitions of multiple reaction monitoring (MRM), plus full-scan acquisition from *m/z* 150–1000 (*m/z* 1000 is the upper limit of this instrument in enhanced MS mode). The instrument was operated in atmospheric pressure chemical ionization (APCI) mode, with conditions optimized for vitamin D, using a vaporizer temperature of 250 °C, curtain gas at 40 arbitrary units (a.u.) and sheath gas at 25 a.u. For SIM, *m/z* 379.3 (=$[M+H-H_2O]^+$) and *m/z* 397.3 (=$[M+H]^+$) were used for vitamin D_2 and *m/z* 367.3 (=$[M+H-H_2O]^+$) and *m/z* 385.3 (=$[M+H]^+$) were used for vitamin D_3. For MRM, the first pair of transitions was *m/z* 397.3→*m/z* 379.3 and *m/z* 385.3→*m/z* 367.3 for vitamin D_2 and D_3, respectively. The dehydration product represented the largest product ion in the MS/MS spectra at fairly low collision energies. A second pair of transitions was selected to employ a low intensity peak from vitamin D_3, to demonstrate that MS/MS peaks from the largest to among the smallest in MS/MS spectra all provide satisfactory quantitative results. The second transitions used were *m/z* 397.3→*m/z* 271.2 and *m/z* 385.3→*m/z* 257.2 for vitamin D_2 and D_3, respectively. Additional discussion and typical MS/MS spectra at high and low collision energies are provided in the electronic supplementary material §2.3.1.1. Flow to this instrument came from the straight-through branch of the fourth tee.

Full-scan APCI-MS on TSQ 7000

Flow from the perpendicular outlet of the fourth tee was directed to a TSQ 7000 tandem sector quadrupole mass spectrometer (ThermoElectron Corp., San Jose, CA, USA), using XCalibur 1.2, operated in positive full-scan APCI mode. Source conditions were optimized for triacylglycerols. The vaporizer heater was operated at 400 °C, the capillary heater was at 265 °C, the corona discharge current was 4.0 μA, and sheath and auxiliary gases were set to 35 psi and 10 a.u., respectively. Scans were recorded from *m/z* 150–1950 in 2 s.

ESI-MS^4 on LCQ deca XP

Flow from the perpendicular outlet of the first tee was directed to an LCQ Deca XP ion trap mass spectrometer (ThermoElectron Corp., San Jose, CA, USA), using XCalibur 1.3, operated in positive ESI mode. Electrolyte

solution (described above) was supplied via the perpendicular branch of a tee connected to the grounding union, at a flow rate of 50 μL/min from an ABI 140B solvent delivery module (Applied Biosystems, Foster City, CA, USA), using both channels at 50% to extend the time between syringe refills, and a contact closure supplied to coordinate refilling syringes during the 5 min LC dead volume. An HP 1050 pumping distilled water at 0.1 mL/min was used to flush the source between runs. The ABI 140B and HP 1050 were plumbed through the electronic switching valve on the front of the LCQ Deca XP, as described in detail in the electronic supplementary material §2.3.3.1.

Source conditions were optimized for triacylglycerols, with the heated capillary at 265 °C, sheath gas at 30 a.u., auxiliary gas at 5 a.u., and spray voltage at 5 kV. Scans were obtained from *m/z* 150–2000 for samples and standards, and from *m/z* 150–4000 for the final column cleanup run. Data dependant acquisition was used to obtain MS/MS, MS^3, and MS^4 from the most abundant ion, with a time of 900 ms and isolation width of 2.0 used to produce useful MS^n spectra.

Calculations

All peak areas were manually integrated using: (1) Agilent Chemstation software for UV at 265 nm, UV at 210 nm (when used) and the Corona CAD for vitamin D_2 and D_3; (2) Analyst 1.5.2 for the QTrap 5500 APCI-MS total ion current chromatograms (TICs), SIM, MRM1, and MRM2 of vitamin D_2 and D_3; (3) Xcalibur 1.3 on the LCQ Deca XP for the ESI-MS TICs, Corona CAD, and ELSD signals for TAGs; and 4) Xcalibur 1.2 on the TSQ 7000 for the extracted ion chromatograms (EICs) of vitamin D_2 and D_3, and for the TICs of TAGs.

Quantification of MS data based on integrated areas in TICs is referred to herein as "level 1 quantification," because it is fast, simple, and appropriate for an industrial or commercial setting. This is in contrast to the highly detailed quantification based on integration of every peak in each EIC for all diacylglycerol-like fragment ions, $[DAG]^+$, and protonated molecules, $[M+H]^+$, that we have described previously [8], which is referred to here as "level 2 quantification". Level 2 quantification is much more labor intensive and time consuming and so is not necessary or appropriate for routine analysis in which the objective is primarily to confirm the identities of oils.

All integrated areas were pasted into Microsoft Excel (with data analysis tools installed) spreadsheets, and calibration curves were constructed using the 'linest()' function applied to all standards. For the internal standard (IS) method, the concentrations of vitamin D_3 in the standards were plotted (calculated) versus the ratio of the area of vitamin D_3 to the area of the vitamin D_2 internal standard, as usual. For the external standard (ES) method, the concentrations of vitamin D_3 in the standards were plotted versus the raw areas of vitamin D_3 in the standards. For the "normal" internal standard response factor (iRF) method, the ratio of the area of vitamin D_3 to the area of the vitamin D_2 internal standard from the middle calibrant was used to calculate a response ratio, and the concentration of vitamin D_3 was calculated using the conventional RF equation, given earlier [6] (and given in the electronic supplementary material §2.4.1). For thoroughness, response factors were calculated for each calibrant level (low, mid, and high), and the resulting quantification compared, in the electronic supplementary material §2.4.1. For exhaustive thoroughness, and to demonstrate the robustness of the method, external standard response factors (eRF) were calculated using the three levels of calibrants by simply dividing the raw peak areas of the vitamin D_3 in samples by the raw peak areas of the vitamin D_3 in standards, times the concentrations of the standards. Thus, results for six different response factors (3×iRF and 3×eRF) are given in the electronic supplementary material §2.4.1, with ES, IS, and iRF2 provided in the main text.

The limit of detection (LOD) was calculated from the calibration curve intercept, *b*, plus three times the standard deviation of the lowest calibration standard (0.25 ug/mL), in units of area for the UV ES method and as an area ratio (D_3/D_2) for the UV IS method and all MS methods. The area or area ratio was converted to the concentration LOD using the calibration line equation. The limit of quantitation (LOQ) was calculated from the calibration curve intercept, *b*, plus ten times the standard deviation in the lowest calibration standard (0.25 ug/mL) and was similarly converted to the concentration LOQ.

The integrated area for each gelcap was divided by the oil weight of that gelcap and multiplied by the average weight for that set, so that all gelcaps within a set were compared on an equal weight basis.

Results and discussion

Vitamin D_3 quantification using UV detection

Figure 2 shows the results for UV, Corona CAD and ELSD detectors recorded on the Agilent 1200 system for a 0.5000 μg/mL calibration standard and for a dietary supplement capsule. The chromatograms of the absorbance at 265 nm (Fig. 2A, E) show sharp, narrow, well-resolved peaks with excellent signal-to-noise ratios (S/N) for the vitamin D_2 internal standard and the vitamin D_3 analyte for both the standard and the supplement gelcap. Such well-resolved peaks allowed facile quantification of vitamin D_3, as given in Table 1. The ELSD was not sufficiently sensitive to

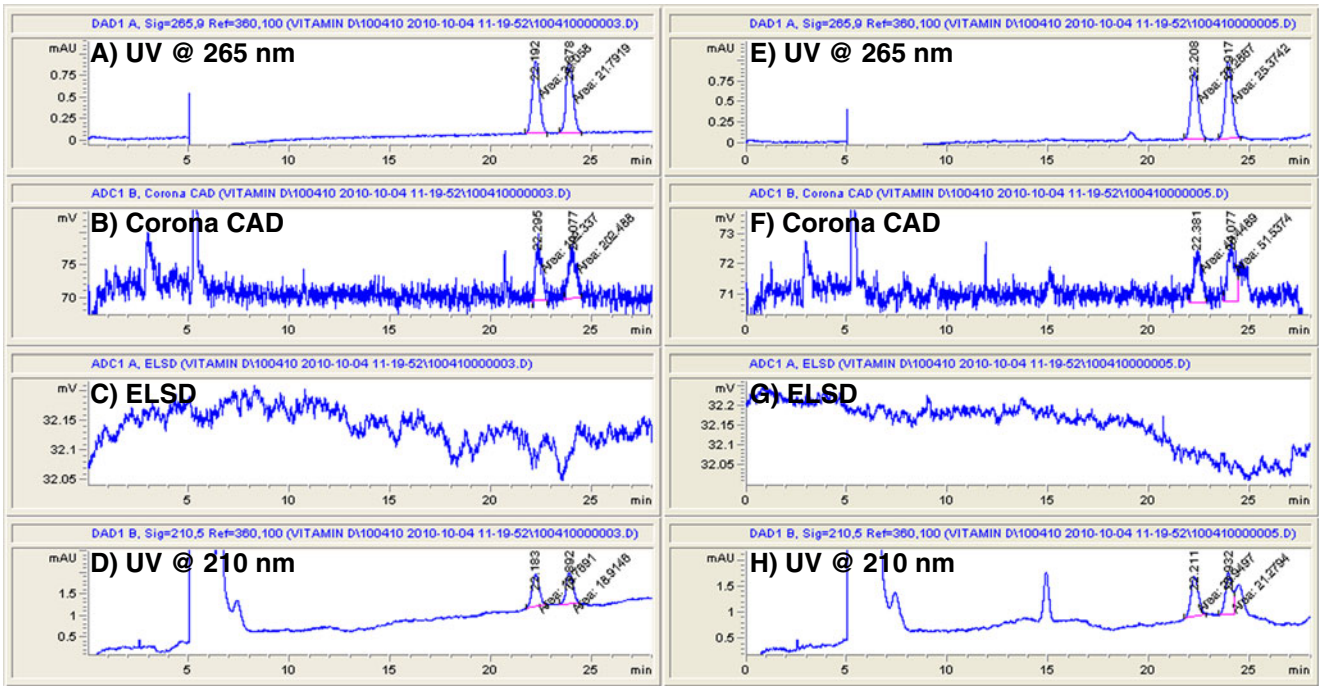

Fig. 2 Agilent 1200 chromatograms from calibration standard (**A**-**D**) and supplement capsule sample (**E**–**H**). **A** UV at 265 nm; **B** corona charged aerosol detector (CAD); **C** evaporative light scattering detector (ELSD); **D** UV at 210 nm; **E** UV at 265 nm; **F** corona CAD; **G** ELSD; **H** UV at 210 nm

produce a usable signal for vitamin D under these conditions. The corona CAD produced visible peaks, but the S/N was not adequate for quantification, and peaks were not distinguishable in all runs. This is because the 20 μL injection of 0.5000 μg/mL solution resulted in 10 ng on the column. These detectors were, however, useful for a comparison of approaches to TAG analysis, described below.

Table 1 presents the data from the UV analysis of 2,000 IU gelcap samples, using IS, ES, and iRF approaches to quantification. The %RSD of the average of three runs for each gelcap was less than 1% in many cases, with a maximum of 1.28% RSD. Furthermore, the average between the five gelcaps was also extremely consistent, with average %RSD values of 0.69%, 0.77%, and 0.77% for the ES, IS, and iRF methods, respectively. The error as expressed by the square root of the sum of the squares (SRSS) of the SDs of the samples is also given in Table 1. The calibration curves showed excellent linearity, with

Table 1 Results (in μg/mL) from UV detection at 265 nm for 50 μg (2,000 IU) vitamin D_3 gelcaps diluted to 100 mL

External standard method			Internal standard method			iResponse factor method		
0.5868[a]	0.0045[b]	0.76%[c]	0.5790	0.0022	0.37%	0.5810	0.0022	0.37%
0.5924	0.0021	0.36%	0.5884	0.0038	0.65%	0.5903	0.0038	0.65%
0.5842	0.0033	0.56%	0.5890	0.0072	1.23%	0.5910	0.0072	1.22%
0.5889	0.0021	0.35%	0.5903	0.0076	1.28%	0.5923	0.0076	1.28%
0.5942	0.0037	0.62%	0.5881	0.0042	0.71%	0.5900	0.0042	0.71%
0.5893[d]	0.0041[e]	0.69%[f]	0.5870	0.0045	0.77%	0.5889	0.0045	0.77%
	0.0073[g]	1.24%[h]		0.0121	2.06%		0.0121	2.06%
LOD	LOQ		LOD	LOQ				
0.0069	0.0229	μg/mL	0.0080	0.0265				

SD in raw D_2 areas, 1.15%

[a] Average of three replicates; [b] Standard deviation of three replicates; [c] %RSD of three replicates; [d] Sample average; [e] SD of five samples; [f] %RSD of five samples; [g] Square root of the sum of the squares (SRSS) of sample standard deviations; [h] %RSD SRSS

correlation coefficients of r^2=0.9996 and 0.9994 for the ES and IS methods, respectively. The LOD from the ES method was 0.0069 μg/mL (27 IU/100 mL) and for the IS method was 0.0080 μg/mL (32 IU/100 mL), for 137 pg and 159 pg on the column, respectively. The LOQ from the ES method was 0.0229 μg/mL (91 IU/100 mL) and for the IS method was 0.0265 μg/mL (106 IU/100 mL), for 457 and 530 pg on the column, respectively.

The UV detector was extremely stable over the full sequence run time, and gave a %RSD in the raw integrated areas of the vitamin D_2 internal standard of only 1.15%, across all standards and samples. Such a high degree of reproducibility provided a means of confirmation that no samples contained any endogenous vitamin D_2. If any sample did contain vitamin D_2, it would immediately be apparent by comparison to the raw integrated areas of the calibration standards, since all standards and samples had exactly 0.5000 μg/mL (2,000 IU) added and produced consistent peak areas.

The internal standard-based response factor method, iRF, reported in Table 1 was calculated from the ratio of the vitamin D_3 to the internal standard in the middle calibrant (1:1 vitamin D_2/D_3), and agreed well with the results produced by the IS three-point calibration curve.

For thoroughness, all permutations of response factors by iRF and eRF approaches were calculated. In addition to the results in Table 1, iRF results were also calculated using the 1,000 IU and 5,000 IU standards. These gave five-sample average values of 0.5811±0.0045 and 0.5879±0.0045 μg/mL, respectively (full results in the electronic supplementary material). External response factors were calculated simply by ratio of the gelcap sample vitamin D_3 areas to the raw areas of the vitamin D_3 in the calibrations standards, giving 5-sample average results of 0.5893±0.0045, 0.5897±0.0041, and 0.5891±0.0041 μg/mL for the eRF approach obtained from the 0.2500, 0.5000, and 1.250 μg/mL standards, respectively.

Although absorbance at 265 nm is the industry standard for vitamin D_3 analysis, absorbance at 210 nm was also selected as a discreet acquisition channel, with the calculated five-sample average amounts being 0.6016±0.0304 (5.06%), 0.6260±0.0249 (3.97%), and 0.6374±0.0243 (3.81%) μg/mL for the ES, IS, and iRF approaches, respectively. The %RSD in the raw vitamin D_2 areas at 210 nm was 7.08%. Obviously, this is not the optimal wavelength for quantification, but even so, the results were comparable to those obtained by other methods, such as MS.

Vitamin D_3 quantification using MS detection

Figure 3 shows the TIC, SIM chromatogram, MRM chromatograms and several mass spectra from the QTrap 5500 instrument, which is newer and much more sensitive than the TSQ and LCQ instruments. It is generally known that SIM is more sensitive than MRM because the ions are formed in the source, whereas MRM requires fragmentation of the precursor, which is not an entirely efficient process. Figure 3 reflects this fact, as seen by the maximum signal levels seen in the SIM (Fig. 3D) and MRM (Fig. 3F, G) chromatograms. The benefit of MRM is specificity since the precursor→product transition provides definitive confirmation that the $[M+H-H_2O]^+$ ions at *m/z* 379.3 and 367.3 came from the precursors at *m/z* 397.3 and 385.3 for vitamin D_2 and D_3, respectively, for MRM transition 1. Thus, MRM is preferred when the instrument is sufficiently sensitive, but SIM can still be used on less sensitive instruments, with some caution [9].

Table 2 gives the results for MS quantification using ions extracted from the full scans, SIM ions, and the two MRM transitions. The APCI process is inherently noisier and less consistent than UV absorbance, giving a SD of raw integrated areas of vitamin D_2 across all samples and standards of 20.18% (compared to 1.15% for UV). Therefore, the ES method was not used for MS data. The correlation coefficients for the four methods compared in Table 2 were r^2=0.9514, 0.9946, 0.9938, and 0.9910 for the TIC, SIM, MRM1, and MRM2 methods, respectively. Based on the poorer S/N in the TIC (Fig. 3B), and the fact that all background (noise) peaks are included in the integrated area, it is expected and observed that the TIC produced larger SD (9.60% RSD and 16.13% SRSS) than the other methods.

Most three-replicate averages for individual samples gave %RSD in the 2–6% range for SIM and MRM, although one low value for an MRM1 run resulted in a SD of 14.77% for one sample. The sample-to-sample deviation was in the 2.29% to 4.05% range, which is very acceptable for an APCI-MS method. If we consider the value from UV detection at 265 nm from the three-point calibration as the most accurate value, MRM1 and MRM2 produced the closest values to the UV results. MRM1 and MRM2 were within 2.53% and 0.38% of the UV value, while the SIM results were within 4.21% of the UV IS value. Thus, all three MS methods are in good agreement with the UV results, and could be used for determination of vitamin D_3 in dietary supplement gelcaps. However, since MRM2 was specifically chosen to be a small peak to demonstrate the wide range of fragments that can be used for vitamin D_3, in the future we will routinely use *m/z* 259.2, which is a larger peak (next in abundance after *m/z* 367.3; electronic supplementary material) and represents loss of the secosteroid "A" ring by cleavage between carbons 6 and 7 (http://en.wikipedia.org/wiki/Secosteroid), which is analogous to the *m/z* 271.2 peak from vitamin D_2.

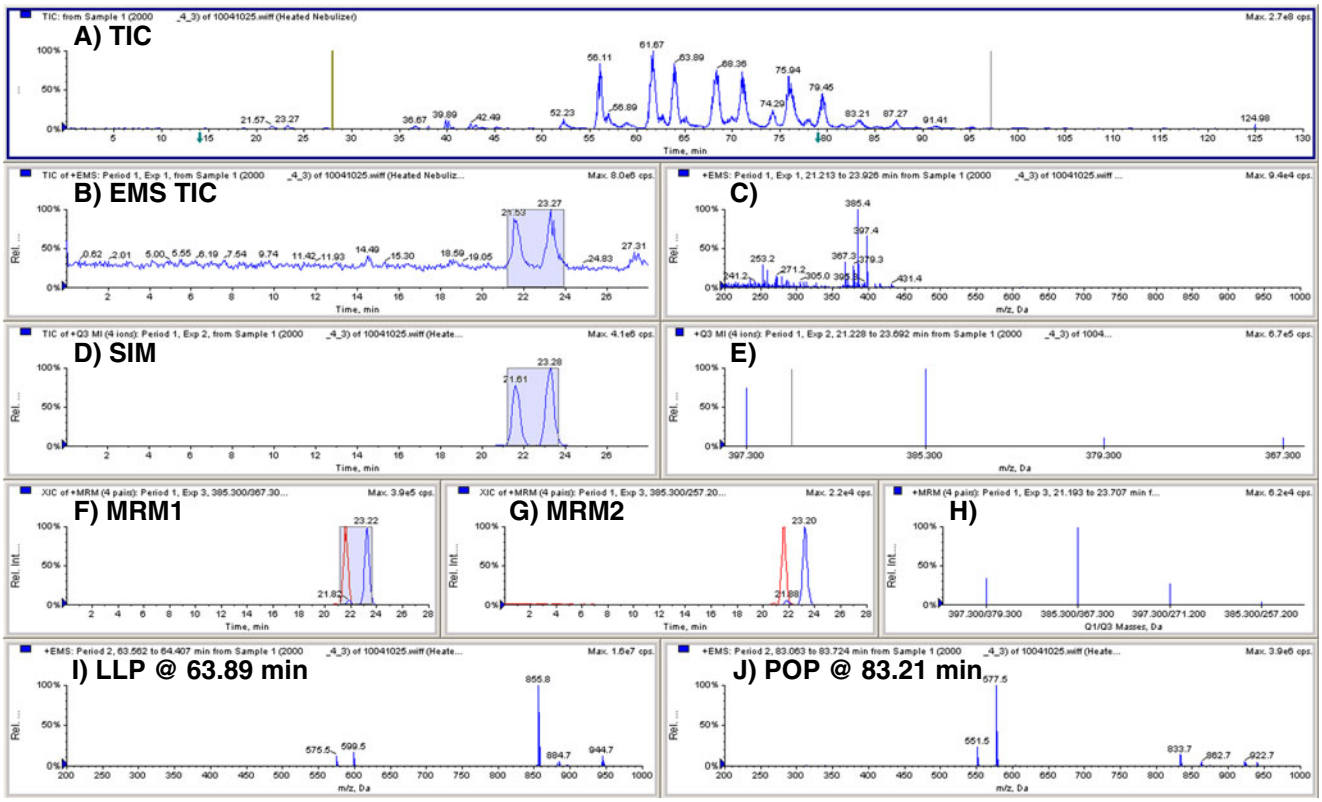

Fig. 3 QTrap 5500 APCI-MS chromatograms and mass spectra. **A** Total ion current chromatogram (TIC); **B** TIC of enhanced MS mode from 0 to 28 min; **C** mass spectrum across vitamin D_2 and D_3 peaks; **D** chromatogram of scans collected in selected ion monitoring (SIM) mode; **E** mass spectrum of SIM ions; **F** chromatogram of ions from multiple reaction monitoring (MRM) transition 1, $[M+H]^+ \rightarrow [M+H-H_2O]^+$; **G** chromatogram of MRM transition 2; **H** mass spectrum of MRM transitions; **I** mass spectrum of peak eluted at 63.89 min; **J** mass spectrum of peak eluted at 83.21 min

The LODs and LOQs by MS are given in Table 2. The MS TIC and MRM1 gave higher estimates, because the % RSDs of the seven replicates of the low standard were 9.52% and 7.35% for these two methods, respectively. These values are higher than most typical %RSDs in Table 2. The SIM and MRM2 data gave %RSDs of 2.81% and 3.79%, respectively, for the data used in the LOD and LOQ calculations from the low standard and calibration curve intercept. The values from these two approaches represent the best estimate of LOD and LOQ values from

Table 2 Results (in μg/mL) from APCI-MS detection on QTrap 5500 for 50 μg (2,000 IU) vitamin D_3 gelcaps diluted to 100 mL

MS			SIM			MRM1			MRM2		
0.5479[a]	0.0166[b]	3.03%[c]	0.6119	0.0174	2.84%	0.6305	0.0362	5.75%	0.5804	0.0177	3.04%
0.6615	0.0804	12.15%	0.6258	0.0133	2.12%	0.5921	0.0271	4.58%	0.5948	0.0306	5.15%
0.5574	0.0317	5.69%	0.5885	0.0352	5.97%	0.5658	0.0538	9.52%	0.5634	0.0832	14.77%
0.5289	0.0127	2.41%	0.6180	0.0191	3.09%	0.6069	0.0147	2.43%	0.5839	0.0136	2.32%
0.6228	0.0310	4.97%	0.6141	0.0248	4.04%	0.6139	0.0049	0.81%	0.6013	0.0232	3.86%
0.5837[d]	0.0560[e]	9.60%[f]	0.6117	0.0140	2.29%	0.6018	0.0244	4.05%	0.5848	0.0146	2.49%
	0.0941[g]	16.13%[h]		0.0519	8.48%		0.0720	11.97%		0.0943	16.13%
LOD	LOQ		LOD	LOQ		LOD	LOQ		LOD	LOQ	
0.0726	0.2420	μg/mL	0.0249	0.0831	μg/mL	0.0549	0.1829	μg/mL	0.0271	0.0902	μg/mL

[a] Average of three replicates; [b] Standard deviation of three replicates; [c] %RSD of three replicates; [d] Sample average; [e] SD of five samples; [f] %RSD of five samples; [g] Square root of the sum of the squares (SRSS) of sample standard deviations; [h] %RSD SRSS

calibration curve data, and represent an LOD of 0.5 ng on the column for both approaches and LOQs of 1.7 and 1.8 ng on the column, respectively.

Triacylglycerol analysis by ESI-MS, APCI-MS, corona CAD, and ELSD

In the new era of ultra high performance liquid chromatography and faster chromatography on smaller columns, it may seem inappropriate to report a 130 min chromatographic analysis. However, there are several factors that prove the value of this analysis. First and foremost, it must be remembered that all of the time-consuming saponification and extraction have been eliminated and the new analysis is automated to run virtually unattended on the LC1/MS3 system. Furthermore, it must be remembered that previous methods required a preparative chromatography separation followed by fraction collection, sample evaporation and reconstitution, and re-injection for analytical chromatography. Thus, a single 130 min run per sample requires no more time, and less human intervention than the method it replaces, in addition to eliminating sample preparation time.

Perhaps the most important consideration is that all information regarding intact triacylglycerols is lost when the conventional analysis is performed. This new method results in a detailed compositional analysis of the triacylglycerols in the sample, as well as vitamin D, so substantially more information is obtained with less manual effort.

Quantification of rice bran oil TAGs by ESI-MS, CAD, ELSD, and APCI-MS

Applications of ESI-MS for triacylglycerol analysis have been reviewed in detail in the past [10], and Han and Gross have described shotgun lipidomics by ESI-MS/MS in detail [11], so these references are not repeated here. Figure 4 shows the ESI-MS data from the LCQ Deca XP ITMS. Although the primary TAGs are labeled in the TIC in Fig. 4A, many more TAGs have been identified than can be labeled, especially given the fact that many of the peaks represent multiple overlapped species. Despite the complexity of the sample, the separation is sufficient that some peaks represent almost pure TAG species. For example, Fig. 4C, D shows the ESI-MS spectra of dilinoleoyloleoylglycerol (LLO) and dioleoylpalmitoylglycerol (OOP), respectively. It can be seen that the mass spectra are extremely clean, with virtually no undesired adduct formation, and minimal protonated molecule peaks. The clean spectra showing only $[M+NH_4]^+$ and $[DAG]^+$ were extremely important to allow small peaks from overlapping TAGs to be assigned with confidence. MS/MS of the ammonium adduct ions provided product ion spectra having almost exclusively a protonated molecule, $[M+H]^+$, and $[DAG]^+$ fragments, similar to APCI-MS mass spectra.

Figure 4B shows that no peaks were observed for vitamin D in the range 0 to 30 min for either ammonium adducts or protonated molecules that would appear in the range 365 to 420 Da, indicating that vitamin D was not adequately ionized by ESI-MS under these conditions.

Figure 4E shows that the corona CAD chromatogram looked extremely similar to the ESI-MS chromatogram. All peaks were present in similar proportions. This apparent similarity is reflected in the quantitative results. On the other hand, many fewer TAGs were quantified by ELSD than by CAD or ESI-MS.

Table 3 presents the percentage composition obtained by ESI-MS of ammonium adducts, corona CAD, ELSD, and APCI-MS (Fig. 5). Since quantification represents the average of all 15 runs in the sequence, quantification was done on the TICs from the MS data ("level 1 quantification"), instead of the very thorough and more time-consuming approach reported previously [8]. The latter method is preferred for an in-depth analysis of triacylglycerols, as it provides integrated areas for all individual fragments, which can be used to construct critical ratios [12] than can be correlated to the regioisomer composition, degree of unsaturation, etc. ("level 2 quantification").

Table 3 shows that the composition given by the corona CAD agrees very well with the results by ESI-MS, and the results by APCI-MS are also in close agreement for most TAGs. The results by ELSD are not very useful due to the limited number of species detected. The 12 TAGs reported by ELSD represent 77.4% of the TAGs determined by corona CAD. The good agreement of the CAD results to the MS results make it clear that if a two-dimensional detector is to be used in combination with UV detection, the corona CAD is much preferred over the ELSD and gives relative percentage quantitative results similar to MS.

There is a paucity of information describing the TAG composition of RBO by HPLC [13], with or without mass spectrometric detection. Since the previous work separated RBO TAGs by argentation chromatography, providing a separation based on the degree of unsaturation, the detailed composition of individual TAGs cannot be compared.

The smaller peaks following each of the primary peaks in the TICs (Figs. 4A, 5A, etc.) represent a combination of isobaric TAGs (e.g., LLL and OLLn, LLO and OOLn; etc., abbreviations in Fig. 4), TAGs with the same equivalent carbon numbers (ECN=carbon chain length−2×no. of double bonds; e.g., LLL and LLPo=ECN 42; POL and PPoO=ECN 46; etc.), regioisomers, and other isomers discussed below. For this reason, the peak labeled "OLLn" actually represented OLLn+LLL2, so is the one labeled "OLLn+" in Fig. 5. Peaks are labeled with the primary component, and all TIC integrated area was attributed to the

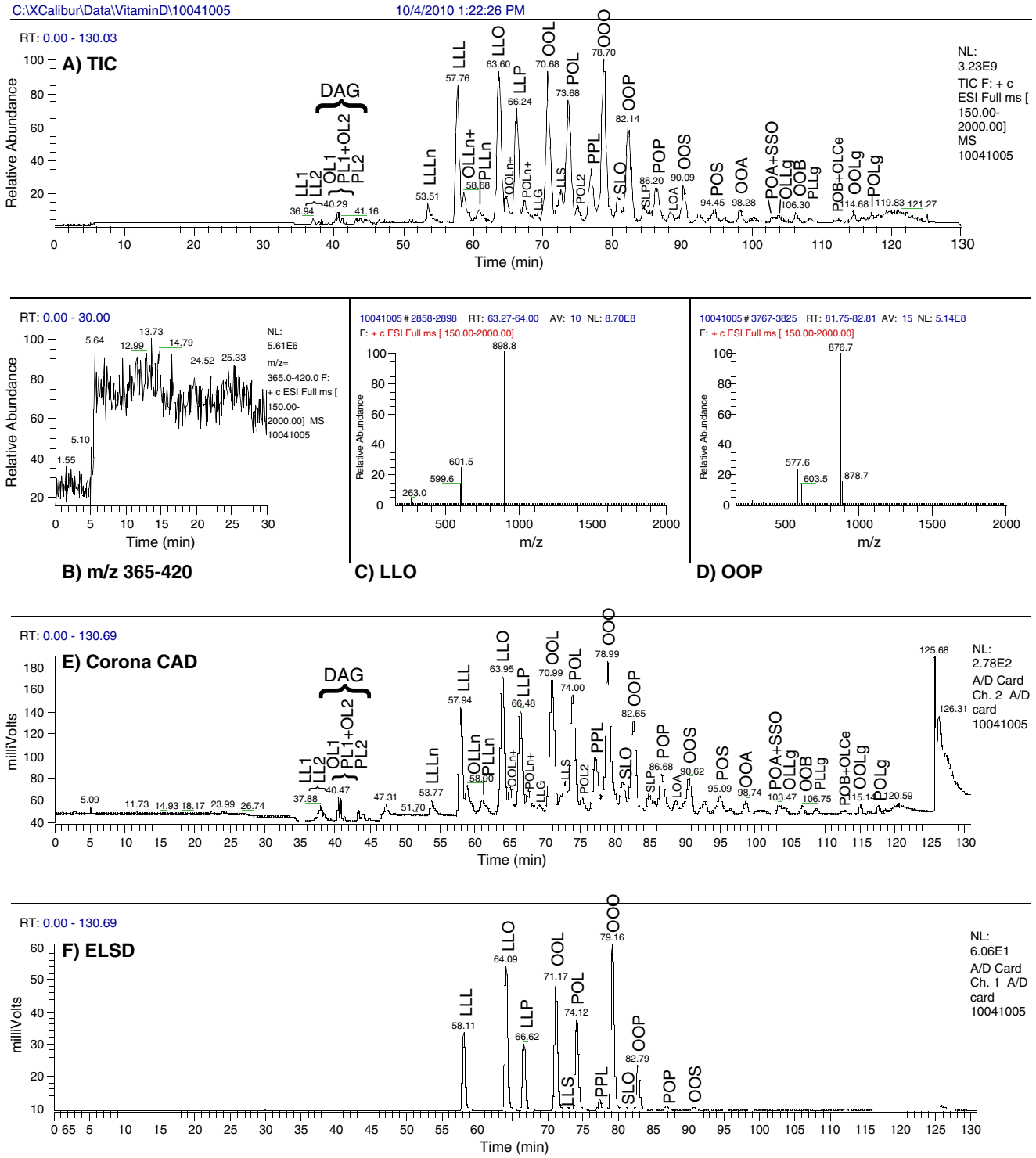

Fig. 4 ESI-MS data from LCQ Deca XP with ammonium formate electrolyte via tee for dietary supplement gelcap containing vitamin D_3 in rice bran oil. Scan range, *m/z* 150 to 2000. **A** TIC; **B** *m/z* 365 to 420 where vitamin D_2 or D_3 would appear; **C** average mass spectrum across peak at 63.60 min; **D** average spectrum of peak at 82.14 min; **E** corona CAD chromatogram; **F** ELSD chromatogram. *P* palmitic (16:0), *Ln* linolenic (18:3), *L* linoleic (18:2), *O* oleic (18:1); *S* stearic (18:0), *A* arachidic (20:0), *B* behenic (22:0), *Lg* lignoceric (24:0)

primary component (e.g., OLLn at 58.46 min in Fig. 5A). Therefore, this and the other primary TAGs in overlapped peaks are expected to be slightly over-represented in the TAG composition.

Double bond isomers of linoleic acid appear to also be present. Comparison of APCI-MS EICs in Fig. 5H–K reveals that secondary peaks occurred for TAGs containing "L." For example, all peaks in the EIC of $[LL]^+$ in Fig. 5H exhibited

Table 3 Percentage compositions of rice bran oil DAGs and TAGs by ESI-MS, CAD, ELSD, and APCI-MS

	ESI-MS TIC		CAD		ELSD		APCI-MS TIC	
	Average[a]	SD	Average	SD	Average	SD	Average	SD
LL1	0.1%	0.1%					0.6%	0.2%
LL2	0.1%	0.0%[b]					0.4%	0.1%
OL1	0.2%	0.0%	0.4%	0.0%			0.8%	0.2%
OL2+PL1	0.3%	0.0%	0.4%	0.0%			0.9%	0.1%
PL2	0.1%	0.0%	0.1%	0.0%			0.3%	0.1%
OO1	0.2%	0.1%	0.3%	0.0%			0.8%	0.1%
OO2+OP1	0.3%	0.1%	0.3%	0.0%			0.9%	0.3%
OP2	0.2%	0.1%	0.1%	0.0%			0.3%	0.2%
LLLn	1.1%	0.1%	1.1%	0.1%			0.9%	0.1%
LLL	6.9%	0.2%	6.0%	0.1%	9.2%	0.3%	6.6%	0.7%
OLLn	1.7%	0.1%	1.7%	0.0%			1.2%	0.2%
PLLn	1.3%	0.1%	1.6%	0.1%			1.1%	0.3%
LLO	10.2%	0.2%	9.1%	0.1%	18.8%	0.2%	10.2%	0.8%
OOLn	1.7%	0.1%	1.8%	0.1%			1.2%	0.2%
LLP	7.7%	0.3%	7.0%	0.2%	8.5%	0.2%	7.9%	0.5%
POLn	1.5%	0.1%	1.8%	0.1%			1.3%	0.3%
LLG	0.6%	0.1%	0.7%	0.1%			0.4%	0.2%
OOL	11.0%	0.2%	10.3%	0.2%	17.5%	0.3%	11.3%	0.5%
LLS	2.5%	0.2%	2.8%	0.2%	0.1%	0.0%	1.8%	0.2%
POL	9.6%	0.2%	9.1%	0.1%	12.8%	0.2%	11.0%	0.5%
POL2	1.0%	0.1%	1.2%	0.1%			0.8%	0.1%
PPL	4.1%	0.1%	4.6%	0.1%	1.4%	0.0%	4.5%	0.2%
OOO	12.7%	0.3%	12.4%	0.3%	24.0%	0.5%	13.5%	0.4%
SLO	2.3%	0.1%	2.4%	0.2%	0.2%	0.0%	1.8%	0.1%
OOP	7.5%	0.2%	7.3%	0.2%	6.6%	0.2%	8.0%	0.4%
SLP	1.2%	0.1%	1.4%	0.1%			1.0%	0.1%
OOG	0.6%	0.1%	0.6%	0.1%			0.4%	0.1%
POP	3.1%	0.1%	3.4%	0.2%	0.5%	0.0%	3.1%	0.2%
OLA	0.9%	0.1%	1.0%	0.1%			0.6%	0.1%
OOS	2.5%	0.1%	3.1%	0.2%	0.3%	0.0%	1.9%	0.1%
SSL+PLA	0.7%	0.1%	1.2%	0.1%			0.7%	0.1%
POS	1.3%	0.0%	1.6%	0.1%			0.9%	0.1%
OLB	0.4%	0.0%	0.4%	0.0%			0.3%	0.1%
OOA	0.9%	0.1%	0.9%	0.0%			0.6%	0.1%
PBL	0.5%	0.1%	0.6%	0.1%			0.3%	0.1%
POA+SSO	0.5%	0.1%	0.5%	0.0%			0.4%	0.1%
OLLg	0.5%	0.0%	0.6%	0.0%			0.3%	0.1%
OOB	0.6%	0.0%	0.5%	0.0%			0.3%	0.0%
PLLg	0.4%	0.0%	0.3%	0.0%			0.2%	0.1%
POB	0.3%	0.1%	0.3%	0.0%			0.2%	0.1%
OOLg	0.5%	0.0%	0.4%	0.0%			0.2%	0.0%
PLCe	0.2%	0.0%	0.1%	0.0%			0.1%	0.0%
POLg	0.3%	0.0%	0.3%	0.0%			0.2%	0.1%
OOCe			0.1%	0.0%				
OOMo			0.1%	0.0%				
	100.0%		100.0%		100.0%		100.0%	

[a]Average of 15 runs, three replicates each for five samples

[b]Less than 0.05%

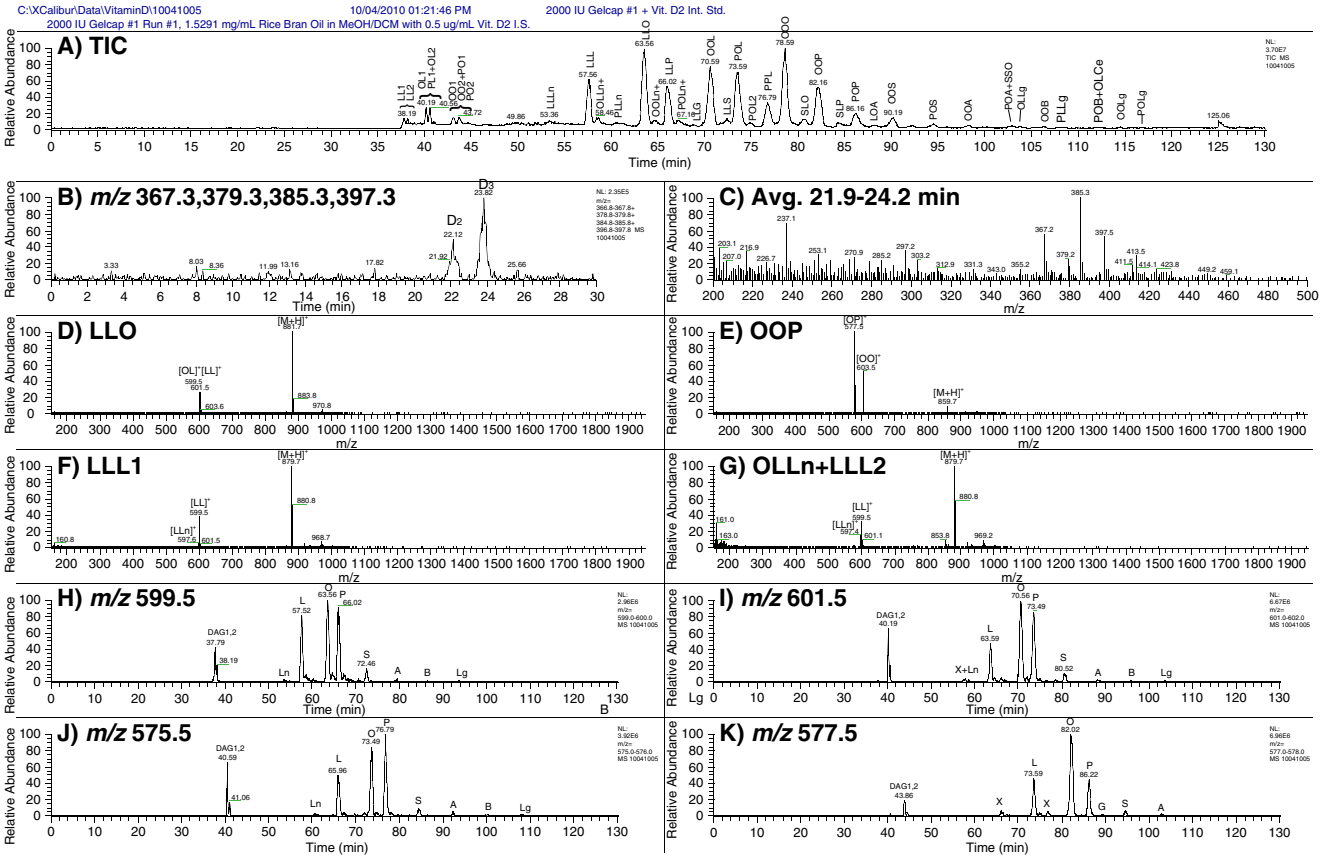

Fig. 5 TSQ 7000 APCI-MS TIC, mass spectra, and extracted ion chromatograms (*EICs*) of TAGs in dietary supplement rice bran oil. **A** TIC; **B** EIC of $[M+H]^+$ and $[M+H-H_2O]^+$ of vitamin D_2 and D_3; **C** average mass spectrum from 21.9 to 24.2 min; **D** average mass spectrum across peak at 63.56 min; **E** mass spectrum across peak at 82.16; **F** average spectrum, 57.2–58.0 min; **G** average spectrum, 58.3–58.9 min; **H** EIC of *m/z* 599.5=$[LL]^+$; **I** EIC of *m/z* 601.5=$[OL]^+$; **J** EIC of *m/z* 575.5=$[PL]^+$; **K** EIC of *m/z* 577.5=$[OP]^+$. Abbreviations in Fig. 4

secondary peaks, whereas only the "L" peak in the EIC of $[PO]^+$ (to give POL) exhibited the secondary peak.

It is important to note that the preference for unsaturated TAGs first reported by Duffin and Henion [14], and exhibited by ESI-MS in our previous report [15] is no longer evident. This may be due to the fact that the higher flow rate (2.5×) of more concentrated (2.5×) ammonium formate more fully saturates the ion spray, eliminating competition between unsaturated and saturated TAGs for ammonium ions, leading to more uniform response across all species. Regardless of the mechanism, the close agreement across the ESI-MS, corona CAD, and APCI-MS results in Table 3 indicates that there is no longer a strong preference for unsaturated species, allowing improved quantification by ESI-MS without response factors.

Quantification of rice bran oil FAs by ESI-MS, CAD, ELSD, and APCI-MS

The FA compositions of various RBOs have been reported [16–21]. Most were determined as fatty acid methyl esters (FAMEs). The FA compositions calculated from the TAG compositions in Table 3 are given in Table 4. When compared to 14 Indian RBOs [20], the FA compositions reported here from TAGs are within the range for every FA except linolenic acid, which was slightly higher (1.90–2.67% in Table 4 versus 0.2–1.6% in Ref. [20]). The difference is, however, small, and will be slightly different when the highly detailed quantification is completed. Stearic acid in Table 4 (2.89–4.36%) was in the range given in Ref. [20] but most reports show a range closer to 1.0–3.0% [13, 16–19, 21]. This, again, is a minor difference. All primary FAs were in good agreement with the cited literature. When the FA compositions in Table 4 are compared side by side with RBO and other oils [16, 18], it is very straightforward to identify the oil as rice bran oil.

Myristic acid was not quantified, because none of the TAGs evident in the TIC contained it. Typical values of the FA are ~0.0–0.4% [13, 17, 18, 20, 21], which is distributed among many TAGs, so each TAG is present at a fraction of that percentage. Despite minor differences in the FA

compositions, the majority of FAs agree well with previously tabulated results.

Identification of rice bran oil VLCFAs by ESI-MS APCI-MS results for TAGs on the QTrap 5500 are not presented, because this instrument was so sensitive that TAGs overwhelmed Q3 in normal mode, leading to errors in centroided masses. The TSQ 7000 was less sensitive and was ideal for APCI-MS analysis of TAGs, as seen in Fig. 5. It produced cleaner APCI-MS spectra, similar to those in the literature. The dependence of APCI-MS on degree of unsaturation meant that no abundant protonated molecule was observed for most VLCFA-containing TAGs since the VLCFAs were mostly saturated, meaning few sites of unsaturation in the overall TAGs. While the $[DAG]^+$ from APCI-MS of VLCFA TAGs on both the QTrap and the TSQ 7000 were helpful for confirmation of the presence of species, the lack of abundant protonated molecule prohibited conclusive identification of these species by APCI-MS alone. Furthermore, the limited mass range of the QTrap 5500 precluded analysis of the VLCFA TAGs with masses above 1000 Da, again highlighting the advantages of having data from other instruments in the multiple parallel mass spectrometry approach.

ESI-MS on the LCQ Deca XP produced $[M+NH_4]^+$ base peaks even for TAGs with few sites of unsaturation, such as OOP shown in Fig. 4D. Figure 6 shows EICs for the most common $[DAG]^+$: $[LL]^+$, $[OL]^+$, and $[OO]^+$, based on the FAs in Table 4. In Fig. 6C, F, I, the small peaks at long retention time are expanded to full scale. Peaks can be seen for arachidic (A=20:0), behenic (B=22:0), lignoceric (Lg=24:0), cerotic (Ce=26:0), and small peaks for montanic (Mo=28:0) acids. Since the peaks for Mo are so small, EICs of the intact $[M+NH_4]^+$ peaks for LLMo, OLMo, and OOMo are given in Fig. 6D, G, J. The retention times and elution orders of these VLCFA TAG species are indicative but not definitive for the presence of the species. The mass spectra in Fig. 7 provide definitive proof of their presence. In each spectrum, the base peak is an intact $[M+NH_4]^+$ ion, with the corresponding $[DAG]^+$ fragments also evident. For example, LLCe in Fig. 7B exhibits the $[M+NH_4]^+$ ion at *m/z* 1012.9, along with the $[LCe]^+$ fragment at *m/z* 715.7 and $[LL]^+$ at *m/z* 599.5. However, across that peak other TAGs, specifically PPS and PLB, are overlapped, giving peaks at *m/z* 852.7 and *m/z* 932.9, respectively. Instead of the average across the breadth of the peak, if a single spectrum near the apex is examined (Fig. 7K), the abundances of the overlapped species are smaller, and the $[M+NH_4]^+$, $[LCe]^+$, and $[LL]^+$ provide more convincing evidence of these species. Similarly, the average spectrum across the LLLg peak (Fig. 7A) may seem confusing, due to overlap of PSO. But the single near-apex spectrum in Fig. 7J clearly indicates the presence of this species. The peaks for Mo in the EICs in Fig. 6C, F, I were very small, and the corresponding spectra in Fig. 7C, F, I have overlapped species present in larger amounts that may lead to some doubt of their presence. But the atypical $[DAG]^+$ at *m/z* 743.x and *m/z* 745.x corresponding to $[LMo]^+$ and $[OMo]^+$, and their progression from Fig. 7C–I, as well as the EICs in Fig. 6D, G, J, are supportive of their presence. Most importantly, the near-apex spectrum in Fig. 7L is definitive for OOMo. Thus, the ESI-MS data provided $[M+NH_4]^+$ and $[DAG]^+$ ions from VLCFA TAGs that allowed these species to be identified as intact TAGs by RP-HPLC-MS of RBO.

Although it should be easier to identify FAs as FAMEs by GC, since FAs from all TAGs are concentrated into a single FA peak, these species have not been reported using GC of RBO. While FAs up to 20:0 have been identified previously [16, 19, 20], no 22:0, 24:0, 26:0, or 28:0 FAs have been reported. This may be due to several reasons: (1) GC-FID is not as sensitive as ESI-MS, even when all FAs are concentrated into one FA peak; (2) such long-chain FAMEs may not elute at a temperature allowed by the GC column upper limit; (3) standards for such VLCFAs are not usually included in standards mixtures; and (4) since they are not usually reported, researchers often do not look for them.

Table 4 Fatty acid composition calculated from TAG compositions in Table 3

FA	ESI-MS	CAD	APCI-MS	ELSD
P	16.20%	16.71%	16.67%	10.55%
Ln	2.45%	2.67%	1.90%	0.00%
L	33.98%	32.46%	34.23%	38.15%
O	41.29%	41.17%	42.79%	51.08%
S	3.68%	4.36%	2.89%	0.22%
A	0.80%	0.93%	0.59%	0.00%
G	0.40%	0.43%	0.26%	0.00%
B	0.60%	0.62%	0.35%	0.00%
Lg	0.54%	0.55%	0.29%	0.00%
Ce	0.05%	0.07%	0.03%	0.00%
Mo	0.00%	0.02%	0.00%	0.00%
	100.00%	100.00%	100.00%	100.00%

TAG and glycerin oligomers by ESI-MS

At the higher dichloromethane percentages and long retention times required to elute VLCFA-containing TAGs, dimers of normal TAGs started to elute, as evidenced by the peaks in the *m/z* 1745 to 1785 range seen in mass spectra in Fig. 7, especially Fig. 7I, J. We have previously demonstrated the sensitivity of ESI-MS to underivatized TAG dimers [15, 22], oligomers [22], and other oxidation products (TAGOX) monomers. Around the same time, van de Berg et al. [23] reported the presence of dimers and trimers from

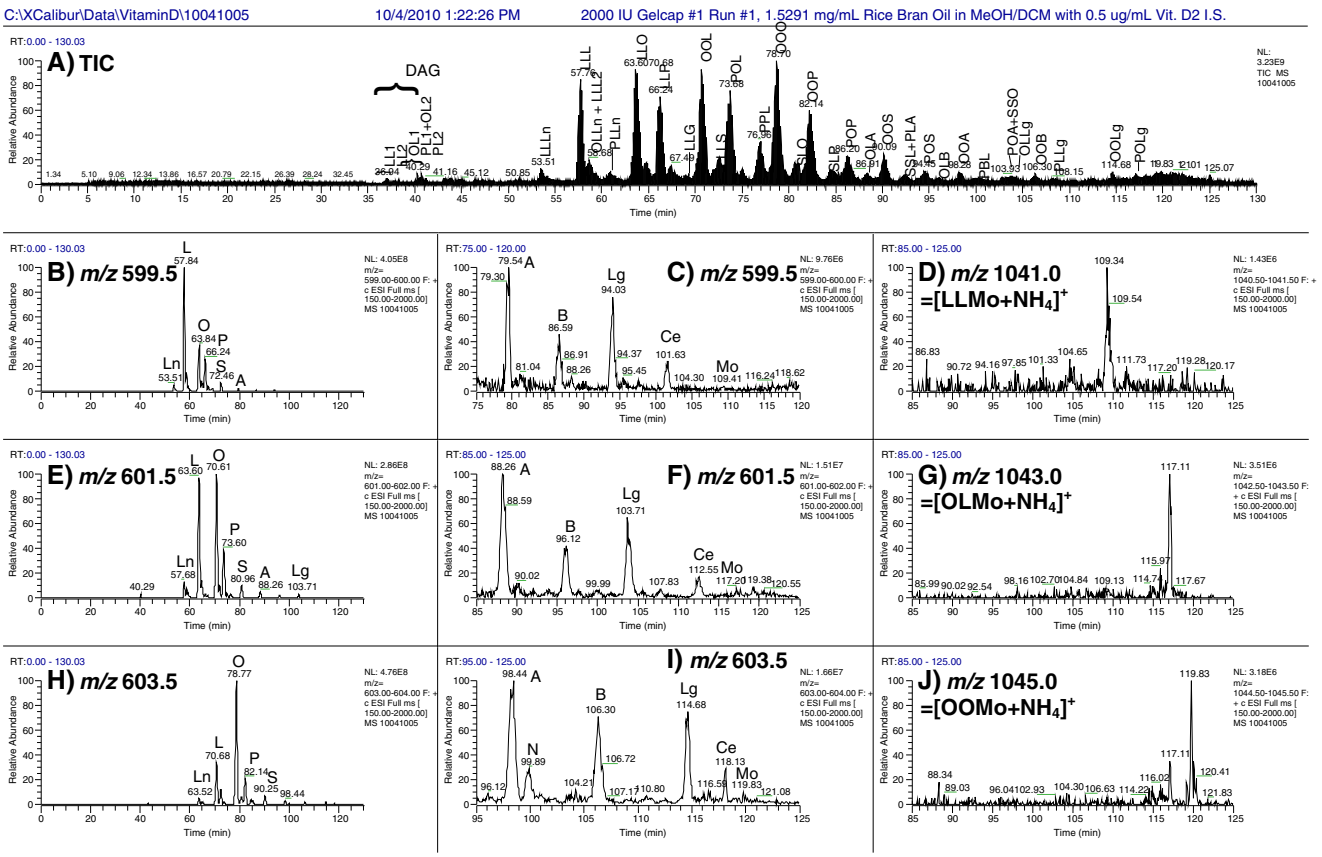

Fig. 6 TIC and extracted ion chromatograms (EICs) of TAGs in dietary supplement rice bran oil. **A** TIC showing all scans; **B** EIC of *m/z* 599.5=$[LL]^+$; **C** EIC of *m/z* 599.5 from 75 to 120 min; **D** EIC of *m/z* 1041.0=$[LLMo+NH_4]^+$; **E** EIC of *m/z* 601.5=$[OL]^+$, **F** EIC of *m/z* 601.5 from 85 to 125 min; **G** EIC of *m/z* 1,043.0=$[OLMo+NH_4]^+$; **E** EIC of *m/z* 603.5=$[OO]^+$; **F** EIC of *m/z* 603.5 from 95 to 125 min; **G** EIC of *m/z* 1045.0=$[OOMo+NH_4]^+$. *N* nervonic (24:1), *Ce* cerotic (26:0), *Mo* montanic (28:0); other abbreviations in Fig. 4

linseed oil by ESI-FTICRMS, and others have also used ESI-MS for analysis of TAGOX monomers [24–28].

The peak pattern from *m/z* 1775.9 to 1783.8 indicates the presence of carbon-linked dimer ammonium adducts, $[(2\times TAG)-2H+NH_4]^+$ or $[(2\times TAG)+NH_4]^+$, that are combinations of OOL, LLO, and LLL. Obviously, the peaks at *m/z* 26 to 28 lower include palmitic acid in one of the TAGs (e.g., PLL and POL).

Since it became apparent that dimers eluted at the end of individual runs, it was expected that larger oligomers were also formed that did not elute during individual runs. Therefore, a column cleaning run was used at the end of the sequence during which ions were monitored up to *m/z* 4000. This final run exhibited peaks and mass spectra (not shown) corresponding to trimers and tetramers, similar to what we have reported previously [22]. Also in those spectra appeared high molecular species having a difference of *m/z* 74 between ions. Based on (1) the fact that the dietary supplement label identified glycerin (glycerol), as well as gelatin, as an ingredient in the gelcaps, and (2) the work of Crowther et al. [29] that described ESI-MS to identify polyglycerols, the peaks differing by *m/z* 74 can be identified as covalently linked HMW glycerol polymers.

A series of smaller polymeric glycerols exhibiting the same difference of *m/z* 74 were evident as a series of chromatographically resolved peaks in run no. 14 and run no. 27 in the 35-run sequence. The polymeric glycerols appeared to elute primarily during the methanol gradient used for vitamin D, but it took many runs for these species to work their way down the columns. Figure 8A shows the chromatogram of distinct peaks arising from smaller polyglycerols. The spectra in Fig. 8 for peaks 1 through 12 distinctly show the progression of peaks by *m/z* 74. The spectra in Fig. 8 are clean and simple compared to APCI-MS data for the same molecules.

Chromatograms and spectra from the QTrap 5500 are provided in Fig. S5 in the electronic Supplementary Material, but the limited mass range of that instrument showed no protonated molecules for peaks 9 through 12, and the $[M+H]^+$ was not the base peak for any of the species. That instrument also showed substantial fragmentation of all species, with all spectra looking similar, and being differentiable primarily by the $[M+H]^+$ and

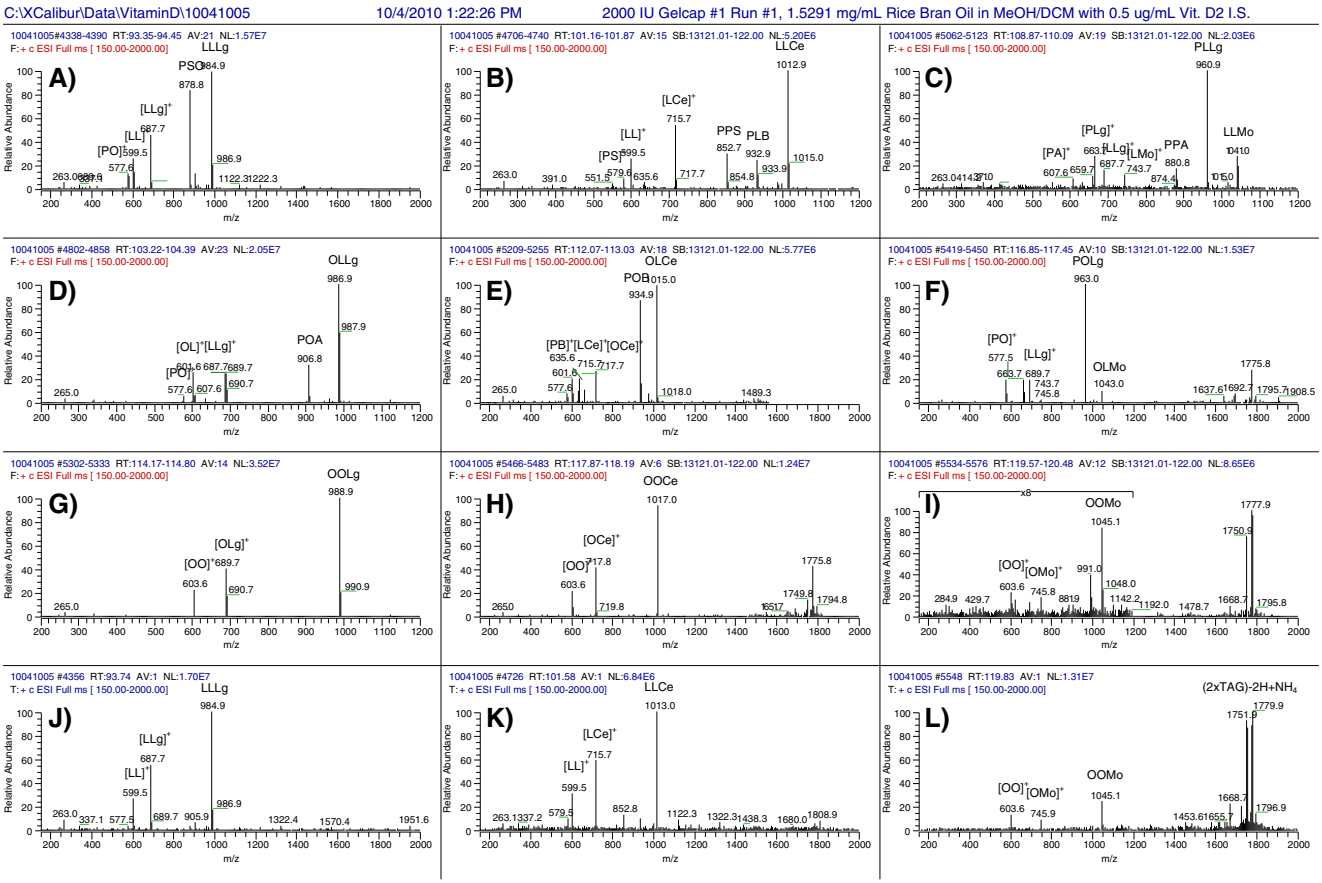

Fig. 7 ESI-MS spectra of TAGs containing VLCFAs, from 24:0 to 28:0. **A**–**I** Average mass spectra across peaks in Fig. 6. **J**–**L** Individual mass spectra. TAG identities labeled above $[M+NH_4]^+$ ions. Peak retention times can be seen in each frame

$[M+H-H_2O]^+$. Overall, the APCI-MS spectra on the QTrap 5500 were not sufficiently useful to be included in the main body of this report.

Since no chemical treatment was applied to the gelcaps prior to analysis (the oil was simply drawn out), these polyglycerols cannot be construed to be artifacts of sample preparation.

Vitamin D_3 from fish oil

For this analysis, dietary supplements were purchased that contained different oils, and also vitamin D_3 from different sources, including synthetic and from fish oil. Figure 9A shows the ESI-MS TIC from a 1,000 IU dietary supplement in safflower oil, with vitamin D_3 from fish oil, obtained using a 95-min gradient (not shown), which used the same initial isocratic methanol. In this figure, three early eluting peaks can be seen, which are expanded in Fig. 9C, the mass spectra of which are given in Fig. 9F–H. These spectra show several differences to later eluting peaks. The spectra exhibit pronounced sodium adducts, $[M+Na]^+$, as well as the $[M+NH_4]^+$ peaks, due to the fact that the elution solvent is 100% methanol, prior to the acetonitrile/dichloromethane gradient. These spectra also exhibit sodium adducts of dimers formed in the ion source, $[(M\times2)+NH_4]^+$. Such dimers are distinct from covalently linked dimers, which are chromatographically resolved from their TAG monomers. The $[DAG]^+$ fragments provided a facile means of identification of this series of TAGs as CyCyCy (tricaprylin, Cy), CyCyCa (caprylic,caprylic,capric), and CaCaCy (capric, capric, caprylic) triacylglycerols.

The CaCaCy eluted at the same retention time as vitamin D_2 but did not share any ions in common with vitamin D_2, so did not interfere with quantification. On the other hand, the CaCaCy peak in the corona CAD chromatogram (Fig. 9L) did preclude quantification of vitamin D by this detector.

Since the MS detector allowed conclusive identification of the potential interferent as CaCaCy, which is not a UV chromophore, it proved that the SCFA TAGs did not interfere with quantification by UV detection at 265 nm. Thus, the ESI-MS data provided confidence in the quantification given by UV at 265 nm. Of course, the information regarding the SCFA TAGs would be lost by saponification of the sample, which probably accounts for the fact that the differences in the sources of vitamin D_3

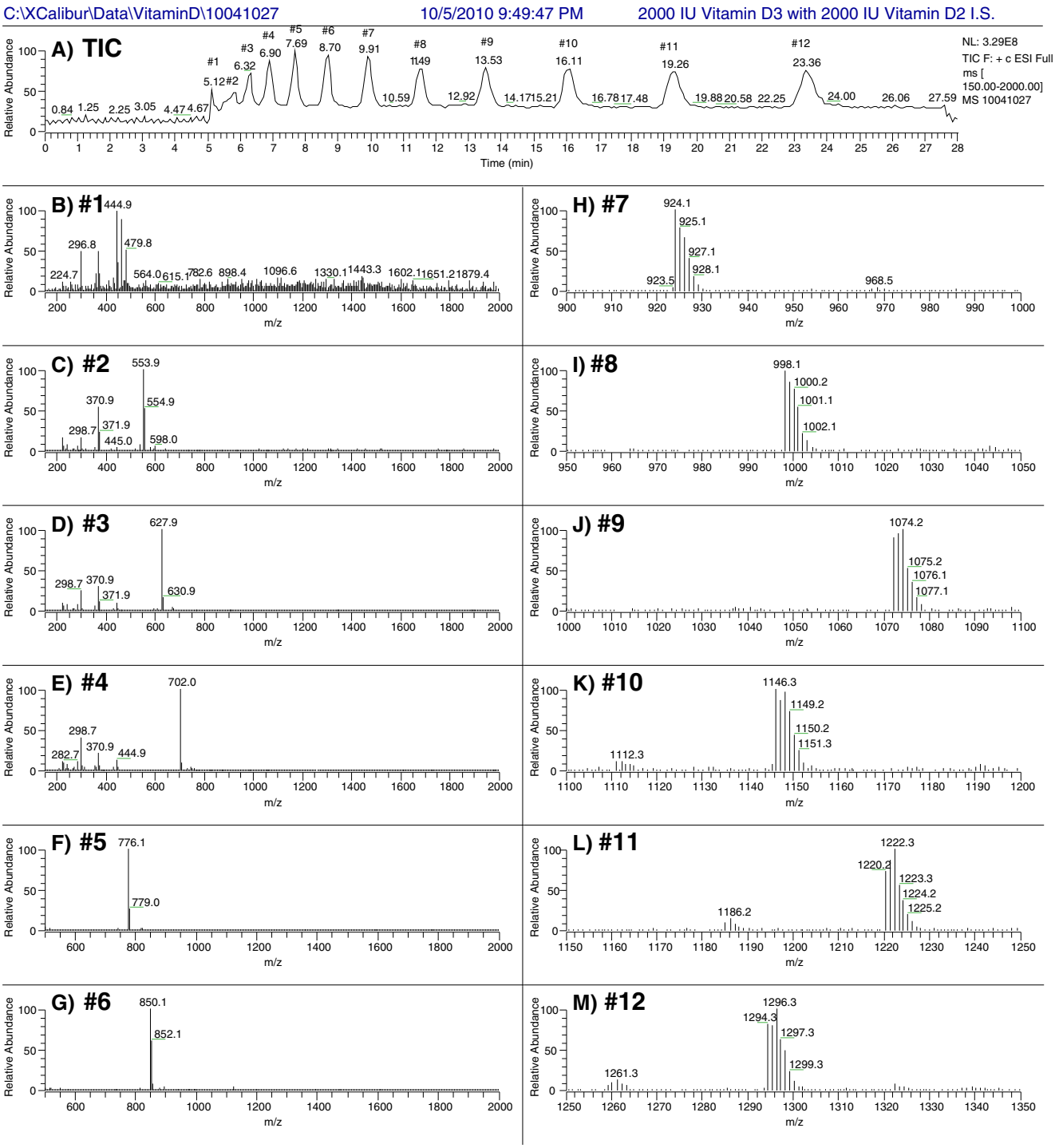

Fig. 8 Polyglycerols in sequence run no. 27, the middle calibration standard (2,000 IU) in the fifth set of bracketed standards. Similar peaks in run no. 14

(synthetic versus from fish oil) have not been previously reported.

Figure 9I–K shows typical safflower oil TAGs from polyunsaturated (LLL) to almost completely saturated (SSO), with the typical $[M+NH_4]^+$ base peaks for all TAGs. Figure 9B shows the EIC for *m/z* 1014.9, which represents several isobaric species containing VLCFAs, overlapped with *m/z* 960.8 (PLLg+OOB, etc.), as seen in the mass spectra (Fig. 9D, E), across the peak at 92.18 min.

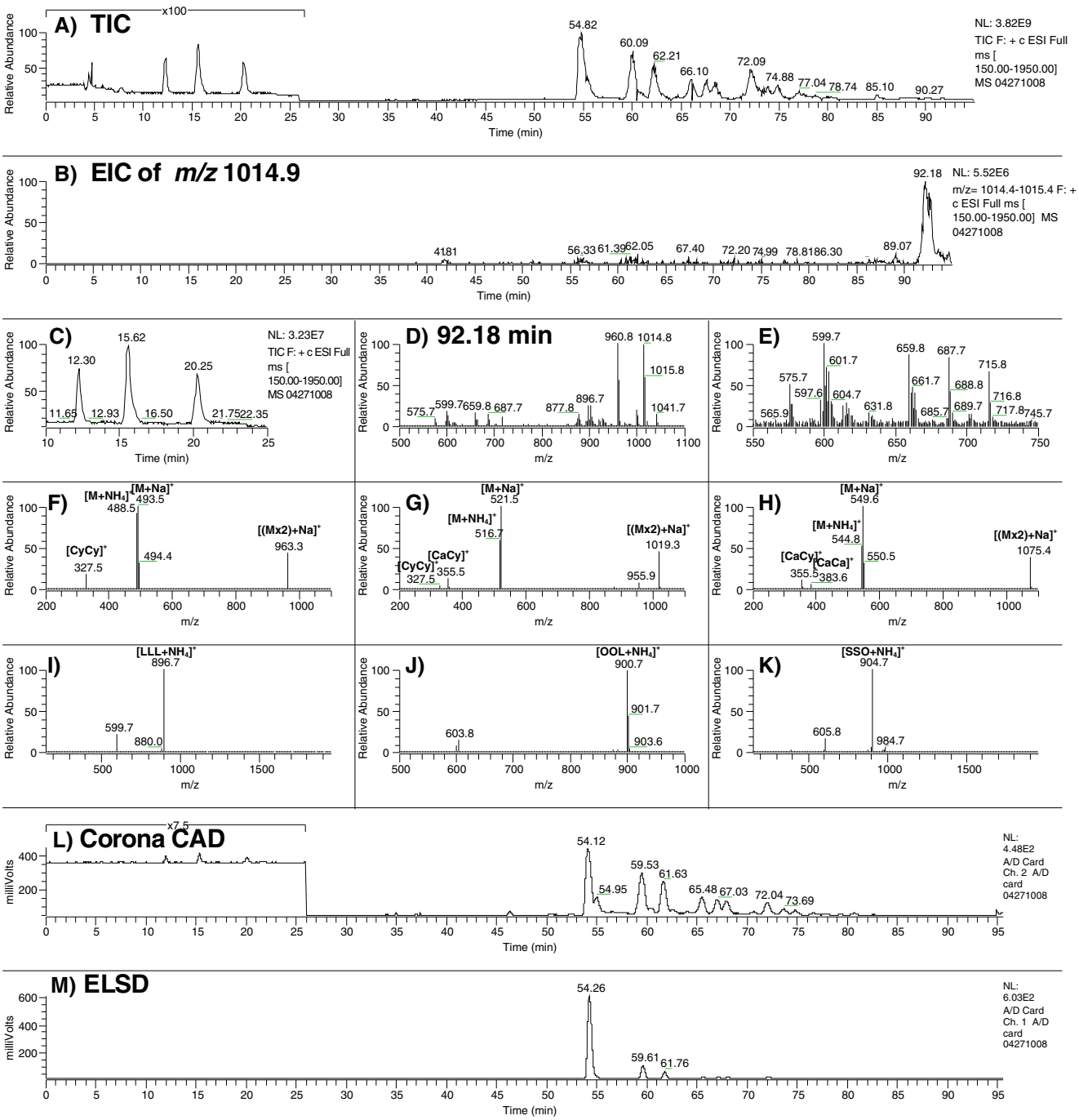

Fig. 9 ESI-MS, Corona CAD and ELSD data for 1,000 IU gelcap in safflower oil with vitamin D_3 from fish oil. **A** ESI-MS TIC; **B** EIC of *m/z* 1014.9; **C** TIC from 10 to 25 min; **D** average mass spectrum across peak at 92.18 min in (**B**); **E** *m/z* range, 550–750 in (**D**); **F** average spectrum across peak at 12.30 min in (**C**); **G** average spectrum at 15.62 in (**C**); **H** average spectrum at 20.25 in (**C**); **I** average spectrum at 54.82 min; **J** average spectrum at 67.63 min; **K** average spectrum at 85.10 min; **L** corona CAD chromatogram; **M** ELSD chromatogram

Conclusions

Reported here is a "dilute-and-shoot" method for analysis of vitamin D_3 in dietary supplement gelcaps that requires minimal sample preparation. The method may be used for external standard, internal standard, and response factor approaches. UV data showed very low standard deviations, often less than 1%, and is the preferred method for sensitive

analysis, as long as mass spectrometry is used to confirm the lack of interfering species. The acquisition of full-scan UV spectra is also recommended for additional verification of the quality of data for quantification, and acquisition of 210 nm is also useful. APCI-MS by SIM or MRM provided sensitive quantification, although standard deviations were higher, usually in the 2–6% range. Results by MS agreed well with results by UV detection. All vitamin D_3-containing dietary gelcaps contained more than the label amount of vitamin D_3, indicating that these are a generally reliable source for dietary vitamin D_3.

Among novel findings reported here are:

- The use of "triple parallel mass spectrometry", with six detectors overall, for triacylglycerol analysis.
- The composition of rice bran oil TAGs by ESI-MS, APCI-MS and corona CAD detection (ELSD identified fewer TAGs).
- Identification of very long-chain fatty acids, up to 28:0.
- Identification of triacylglycerol oligomers (dimers, trimers, and tetramers) at low levels.
- Identification of glycerol oligomers in dietary supplement gelcaps.
- Identification of SCFA TAG species in gelcaps that used vitamin D_3 from fish oil, which were not found in brands that used synthetic vitamin D_3.

While the reported method uses a 130 min run, the fact that it eliminates saponification and extraction, as well as preparative HPLC, fraction collection and re-injection while at the same time providing extensive knowledge of the triacylglycerol composition and additional novel information, makes it worth the time required for the chromatography.

References

1. DeLuca HF (1988) FASEB J 2:224–236
2. Chung M, Balk EM, Brendel M, Ip S, Lau J, Lee J, Lichtenstein A, Patel K, Raman G, Tatsioni A, Terasawa T, and Trikalinos TA (2009) Evid Rep Technol Assess (Full Rep)1-420
3. Holick MF (2006) Mayo Clin Proc 81:353–373
4. Institute of Medicine Food and Nutrition Board (2010) Dietary reference intakes for calcium and vitamin D. National Academy Press, Washington, DC
5. Webb AR, Kline L, Holick MF (1988) J Clin Endocrinol Metab 67:373–378
6. Byrdwell WC (2009) J Agric Food Chem 57:2135–2146
7. Bartolucci G, Giocaliere E, Boscaro F, Vannacci A, Gallo E, Pieraccini G, Moneti G (2011) J Pharm Biomed Anal 55:64–70
8. Byrdwell WC, Neff WE, List GR (2001) J Agric Food Chem 49:446–457
9. Byrdwell WC, Exler J, Gebhardt SE, Harnly JM, Holden JM, Horst RL, Patterson KY, Phillips KM, Wolf WR (2011) J Food Compos Anal 24:299–306
10. Byrdwell WC (2005) Qualitative and quantitative analysis of triacylglycerols by atmospheric pressure ionization (APCI and ESI) mass spectrometry techniques. In: Modern methods for lipid analysis by liquid chromatography/mass spectrometry and related techniques. AOCS Press, Champaign, IL
11. Gross RW, Han X (2009) Am J Physiol Endocrinol Metab 297: E297–E303
12. Byrdwell WC (2005) Lipids 40:383–417
13. Denev R, Kuzmanova I, Panayotova S, Momchilova S, Kancheva V, Lokesh BR (2009) C R Acad Bulgare Sci 62:709–716
14. Duffin KL, Henion JD, Shieh JJ (1991) Anal Chem 63:1781–1788
15. Byrdwell WC, Neff WE (2002) Rapid Commun Mass Spectrom 16:300–319
16. Karmakar A, Karmakar S, Mukherjee S (2010) Bioresour Technol 101:7201–7210
17. Reena MB, Krishnakantha TP, Lokesh BR (2010) Prostaglandins Leukotrienes Essent. Fatty Acids 83:151–160
18. Bhatnagar AS, Prasanth Kumar PK, Hemavathy J, Gopala Krishna AG (2009) JAOCS J Am Oil Chem Soc 86:991–999
19. Jennings BH, Akoh CC (2009) J Agric Food Chem 57:3346–3350
20. Gopala Krishna AG, Hemakumar KH, Khatoon S (2006) JAOCS J Am Oil Chem Soc 83:117–120
21. Bravi E, Perretti G, Montanari L (2006) J Chromatogr A 1134:210–214
22. Byrdwell WC, Neff WE (2004) JAOCS J Am Oil Chem Soc 81:13–26
23. van den Berg JDJ, Vermist ND, Carlyle L, Holcapek M, Boon JJ (2004) J Sep Sci 27:181–199
24. Tarvainen M, Suomela JP, Kuksis A, Kallio H (2010) Lipids 45:1061–1079
25. Suomela JP, Ahotupa M, Kallio H (2005) Lipids 40:437–444
26. Suomela JP, Ahotupa M, Sjovall O, Kurvinen JP, Kallio H (2004) Lipids 39:639–647
27. Giuffrida F, Destaillats F, Skibsted LH, Dionisi F (2004) Chem Phys Lipids 131:41–49
28. Suomela JP, Ahotupa M, Sjovall O, Kurvinen JP, Kallio H (2004) Lipids 39:507–512
29. Crowther MW, O'Connell TR, Carter SP (1998) JAOCS J Am Oil Chem Soc 75:1867–1876